

ENHANCEMENT OF COMPLEX PERMITTIVITY AND ATTENUATION PROPERTIES OF ACTIVATED CARBON DERIVED FROM OIL PALM FRUIT FIBER FOR MICROWAVE APPLICATION

*¹Ismail Ibrahim Lakin, ¹Asiya Hassan, ²Rabi'u Abubakar Tafida, ¹Nicodemus Kure, ¹Gyuk Philibus Musa, ³Ibrahim Garba Shitu

¹Department of Physics, Faculty of Science, Kaduna State University, Kaduna, Nigeria

²Department of Physics, Nigerian Defence Academy, Afaka, PMB 2109, Kaduna, Nigeria

³Department of Physics, Faculty of Science, Sule Lamido University, Kafin Hausa, Jigawa State, Nigeria

*Corresponding Author Email Address: ismaillakin59@gmail.com

Phone: +2348037245036

ABSTRACT

This study aimed to synthesize activated carbon (AC) from empty oil palm fruit bunch (OPEFB) fiber to enhance its complex permittivity properties by modifying the particle size and surface area via physical activation. Sample characterizations of complex permittivity were conducted using open-ended coaxial technique and a vector network analyzer. The absorption properties were analyzed using the finite element method (FEM) simulations of the transmission coefficients and the distribution of electric fields via the microstrip models. Simulations and measurements were all carried out within the range 8–12 GHz. The initial surface area of the unactivated sample was 4.02, after 700, 750, and 800 °C activation, 730.40, 814.00, and 927.01 m²/g was obtained respectively. With increased surface area, the dielectric constant and loss factor values increased and attained maximum values of 6.13 and 0.83 at 8 GHz, respectively from initial values of 3.63 and 0.52, as the surface area increased from 4.02 to 927.01 m²/g. The improved absorption properties displayed by the AC in the simulations demonstrated their capacity to attenuate X-band microwaves.

Keywords: Complex permittivity; OPEFB Fiber; Electromagnetic waves; Transmission coefficient; Microwaves

INTRODUCTION

The extensive growth and rapid advancement in communication and electronic devices, problems involving electromagnetic interference (EMI) have continued to increase; hence, the material study of microwave absorbers has received widespread interest. In microwave absorbing applications, different magnetic materials were used, the most common being ferrites owing to their exceptional electrical and magnetic properties. However, Ferrites are expensive, heavy, and have higher complex permittivity (Yang *et al.*, 20016); this implies more reflection; the reflecting characteristic is not good for military defense, as this reflection can be easily tracked by radar. Nonetheless, carbon-based materials (carbon black (CB), activated carbon (AC), carbon nanotubes (CNTs), and recently graphene) were chosen to replace ferrites due to low density, resistance to corrosion, strengthening potential and strong electrical/thermal conductivity (Srivastava *et al.*, 2020; Choh *et al.*, 2016). Agricultural waste is regarded as a very significant precursor since it is inexpensive, reusable, safe abundant, and biodegradable; moreover, it has a high carbon and less ash content (Chayid *et al.*, 2015; Ahmed, 2016; Ooi *et al.*, 2017).

Activated carbon (AC) produced from agricultural wastes such as

rice husk, corn cob, and wheat straw (Ratan *et al.*, 2017), bamboo (Tsubota *et al.*, 2016), coal pitch (Zhong *et al.*, 2016) were successfully synthesized via low-cost technique. Abdalhadi *et al.*, recently reported that compacted oil palm empty fruit bunch (OPEFB) fiber of 200 μm grain size possessed good dielectric properties in the 8-12 GHz range. Using a simple processing technique, modified OPEFB fiber (AC) can be manufactured cheaply, has low environmental waste, and also has peculiar electrical properties. However, the complex permittivity property is enhanced while maintaining dielectric attributes, which may increase the absorption capacity of AC microwaves (Afifah Mahmud *et al.*, 2018).

Surface transmittance, energy absorbance, and energy reflection are the principal effects of the interaction between a dielectric material and an electric field. These effects aid in demonstrating the electrical features of relative permittivity. The relative complex permittivity can be represented by the equation;

$$\epsilon^* = \epsilon' - j\epsilon'' \quad (1)$$

Where ϵ' represents the dielectric constant and ϵ'' the loss factor respectively. Complex permittivity can be measured using several techniques such as a rectangular waveguide and open-ended coaxial (OEC), based on measurements of high frequency. The use of the OEC probe technique for the complex permittivity measurement of powdered and compressed materials has been documented (Abdalhadi *et al.*, 2018; Ibrahim Lakin *et al.*, 2020). However, to the best of our knowledge, the characterization of the complex permittivity of AC derived from OPEFB fiber using the OEC technique is still yet to be examined.

The study aimed to enhance the complex permittivity properties of OPEFB fiber by modifying the surface area for several temperatures through physical activation. The dielectric measurement of the samples was carried out via the OEC probe technique. The transmission coefficients of the samples were numerically calculated utilizing the geometry of the microstrip model using the finite element technique (FEM). The attenuation characteristics were analyzed using simulated transmission coefficient (dB) values and the electric field distributions due to material absorption were also examined.

MATERIALS AND METHODS

Synthesis of AC from OPEFB Fiber

The OPEFB fiber was obtained from Hulu Langat Oil Palm Mill, Dengkil Selangor, Malaysia. It was then prepared for the activation as illustrated in Figure 1. To reduce moisture, the OPEFB fibers were soaked in distilled water for 18h and dried in an oven at 80 °C for 6 h. The dried fibers were crushed into powder, which was then

sifted 100 µm by a laboratory test sieve (Endecotts, London, England). Part of the processed 100 µm OPEFB was used as the raw material to synthesis the AC. The OPEFB fiber was initially carbonized using a drop type pyrolyzer at 450 °C. The carbonized OPEFB fiber was activated, separately for 700, 750, and 800 °C

for 90 mins activation time using a tube furnace at a 20 °C/min heating rate in a flow of nitrogen gas. A carbon dioxide gas (CO₂) was used to activate the sample for 1 h as reported in the study by Osman et al., 2016.



Figure 1. Synthesis of Activated carbon

Textural Characterization

The outer morphology of the samples was examined using field emission scanning electron microscopy FE-SEM (Nova NanoSEM 230, FEI Holland) at a fixed voltage of 10 kV. Energy-dispersive X-ray spectroscopy (EDX) was used to examine the elemental composition of the samples. Finally, AUTOSORB-1 (Quanta Chrome Instruments) were used in determining the surface area. The samples were sonicated at 300 °C under nitrogen for 4 h. Then, the specific surface areas were calculated by Brunauer Emmett, and Teller (BET).

Dielectric Properties Measurement

Using the OEC probe HP85071C (Agilent, Santa Clara, California) approach, measurements of the composites' complex permittivity were made. The OEC probe is well adapted to determining the complex permittivity of liquids (Yakubu et al., 2015). It can, however, be used for solids, but great care should be taken to ensure that the samples are flat and that the sample and probe are in good contact as illustrated in Figure 2.

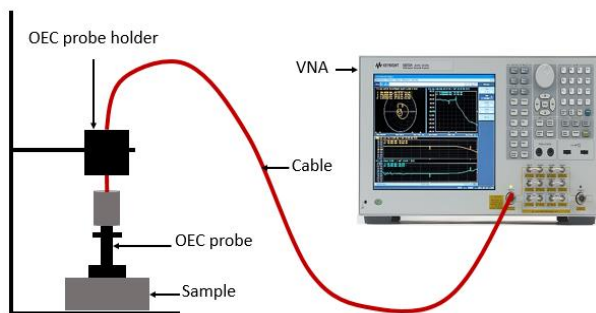


Figure 2. Complex permittivity measurement using OEC

Material Absorption Properties

In this research, the finite element method (FEM) is utilised to simulate a microstrip for microwave characterization. The

simulation is implemented using the COMSOL Multiphysics ® software package, version 3.5. A transmission coefficient $|S_{21}|$ is a parameter that can be directly calculated at microwave frequencies and is complex in terms of magnitude and phase. Often the amplitude is given in decibels (dB), expressed as;

$$dB = -20 \log(S_{mn}) \quad (2)$$

Where $m = 2$, and $n = 1$. Eq. 2 is also called attenuation. Thus, the result obtained via the simulation is then used to calculate the attenuation characteristics of a material for microwave absorption applications.

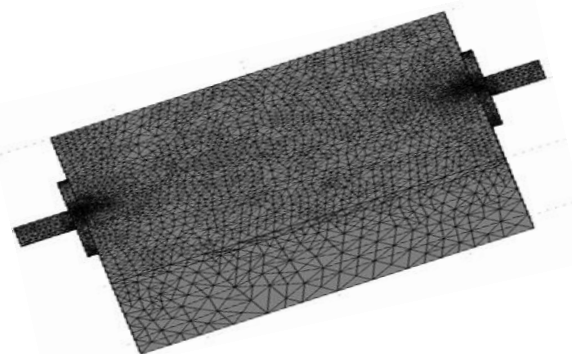


Figure 3. Mesh of microstrip for FEM simulation.

RESULTS AND DISCUSSION

Morphological Characterization

Figure 4 shows the FESEM micrographs of OPEFB fiber and its AC. All the AC samples synthesized at various temperature conditions showed a similar structure under SEM observation (Lee et al., 2014). Thus, only the OPEFB fiber sample micrograph activated at 750 °C was selected to represent the entire AC samples for comparison with the OPEFB fiber. We observed that before the activation the OPEFB fiber (Fig. 4a and c) surface texture was rough, irregular, and found on the surface were a lot of

cavities. The smooth surface of the AC (Fig. 4b and d) was created due to the volatile organic materials such as wax and pectin liberation, and carbon particle densification. This is in agreement with the work-study reported by Lee et al., 2013. The AC image appears to be more compact if compared with the initial OPEFB fiber Structure (external surface). Table 1 shows the activation time and temperature, carbon percentage, and BET surface area of the OPEFB fiber and AC. The BET surface area of the OPEFB fiber

was 4.02 m²/g. However, after 700, 750 and 800 °C of activation, the BET surface areas were respectively, 730.40, 814.00, and 927.01 m²/g. Modification of the OPEFB fiber through carbonization and activation processes produced wide surface area for absorption thus correlated with the literature that is the target in activated carbon processing.

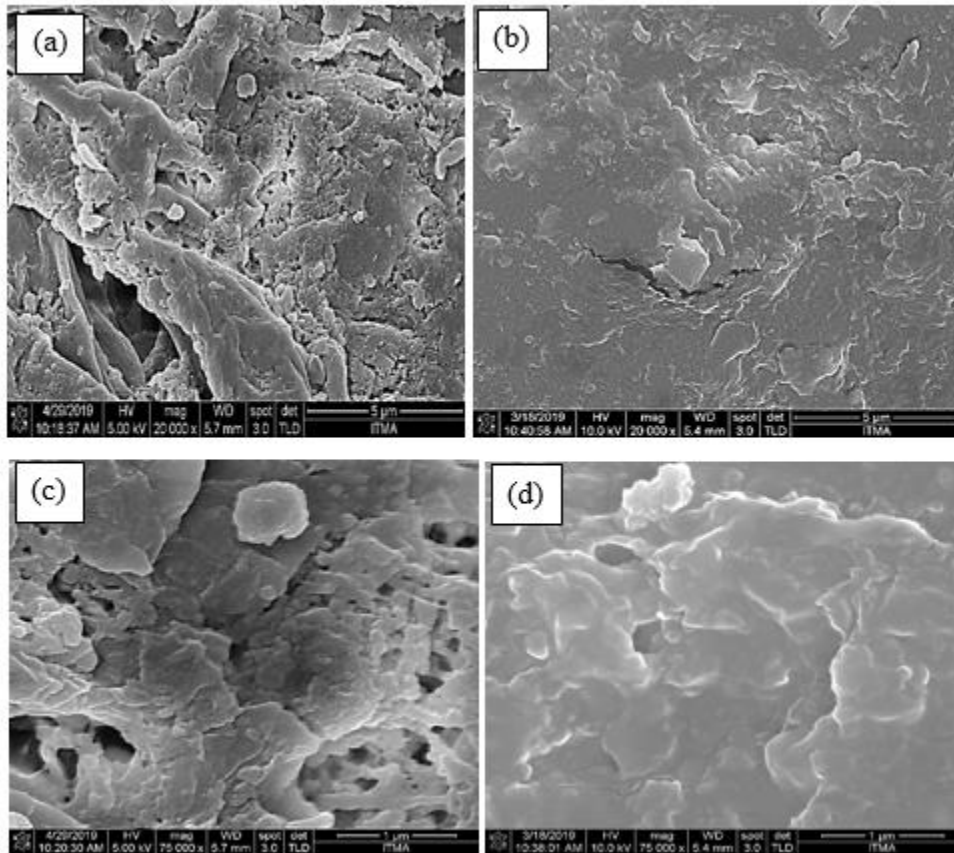


Figure 4. FESEM micrographs of
 (a) OPEFB fiber and (b) AC derived from OPEFB fiber scanned at 5 μm
 (c) OPEFB fiber and (d) AC derived from OPEFB fiber scanned at 1 μm

Table 1. Effect of activation temperature on carbon content (%) yield

Sample	Activation time (min)	Temp (°C)	Carbon (C %)	BET surface area (m ² /g)
OPEFB fiber	-	-	64.11	4.02
AC	90	700	79.02	730.40
	90	750	86.23	814.00
	90	800	92.74	927.01

Figure 5 shows the EDX analysis spectra of the AC and the carbon element contents are tabulated in Table 1. The results displayed that the OPEFB fibers (Fig. 5a) were composed of 64.11 wt%C, 34.99 wt%O with about a 1% of silica as an impurity. Upon activation, the AC activated at 700 °C was observed to have a higher carbon content of 79.02wt% with 20.48 wt%O compared to EFB fiber. After 750 and 800 °C of activation, the C wt% increased to 86.23 and 92.74, while O wt% decreased to 13.72 and 7.22 respectively. As compared to AC activated at 700 and 750 °C respectively, the higher percentage of carbon content in AC activated at 800 °C was attributed to the additional activation temperature. The volatile mineral content was burned off during the activation process and left behind carbon content (Ooi et al., 2013; Wirasnita et al., 2015).

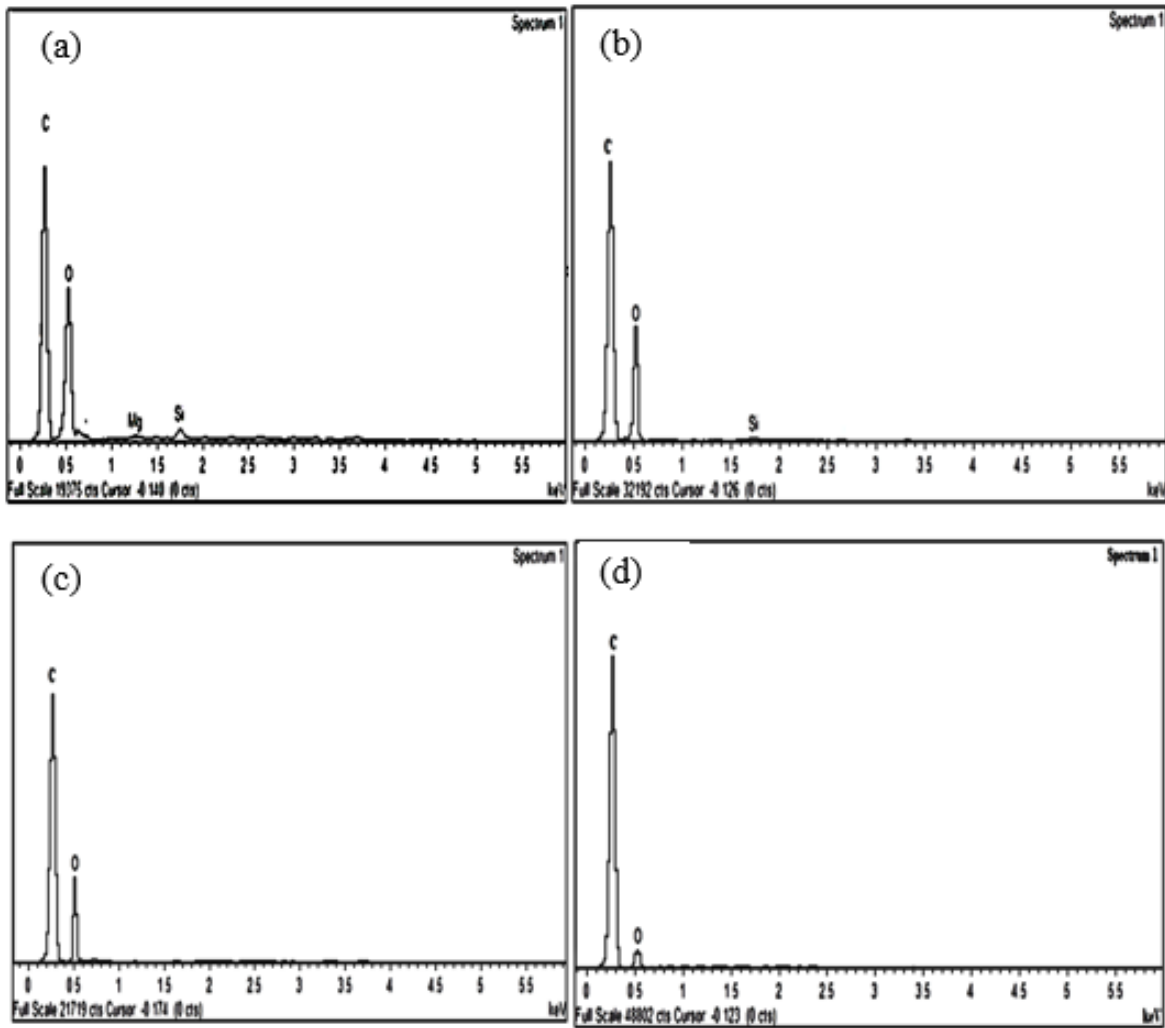


Figure 5. EDX Spectra of OPEFB fiber after (a) 0 °C, (b) 700 °C, (c) 750 °C, and (d) 800 °C of activation

Dielectric Characterization

Figure 6 indicates the frequency variation of ϵ' and ϵ'' for OPEFB fiber activated at 0, 700, 750, and 800 °C. The results revealed that ϵ' and ϵ'' parts of the permittivity significantly increased when the particle size and surface area of the OPEFB fiber were modified by activation. At 8 GHz, ϵ' increased from 3.61 to 6.07, while ϵ'' increased from 0.49 to 0.81 when the surface area was increased from 4.02 to 927.01 m²/g. The sample with the largest surface area, therefore, had the maximum values of complex permittivity. This indicates an enhancement in the complex permittivity of modified surface area OPEFB fiber. It is evident that, ϵ' and ϵ'' for all the samples decreased with increasing frequency.

The significantly higher AC permittivity values can be related to the specific surface area and interface density resulting in increased interfacial polarization (Mensah *et al.*, 2019). Similarly, finer particles (larger surface area) had fewer air gaps, more compact,

and, thus, established good contact between the constituent particles contributing to the noted increase in interface density. Therefore, the resulting interfacial polarization elevated, leading to an increase in dielectric permittivity. At lower frequency, the conductive grains are isolated by thin insulating grain boundaries, which allows a concentration of charges under the influence of the electric field and thus increases the interfacial polarization in a high ϵ' . However, at high frequencies, the charge carrier cannot align themselves in the direction of the electric field leading to decreased interfacial polarization (El Khaled *et al.*, 2018; Sherif *et al.*, 2016; Ibrahim Lakin *et al.*, 2020).

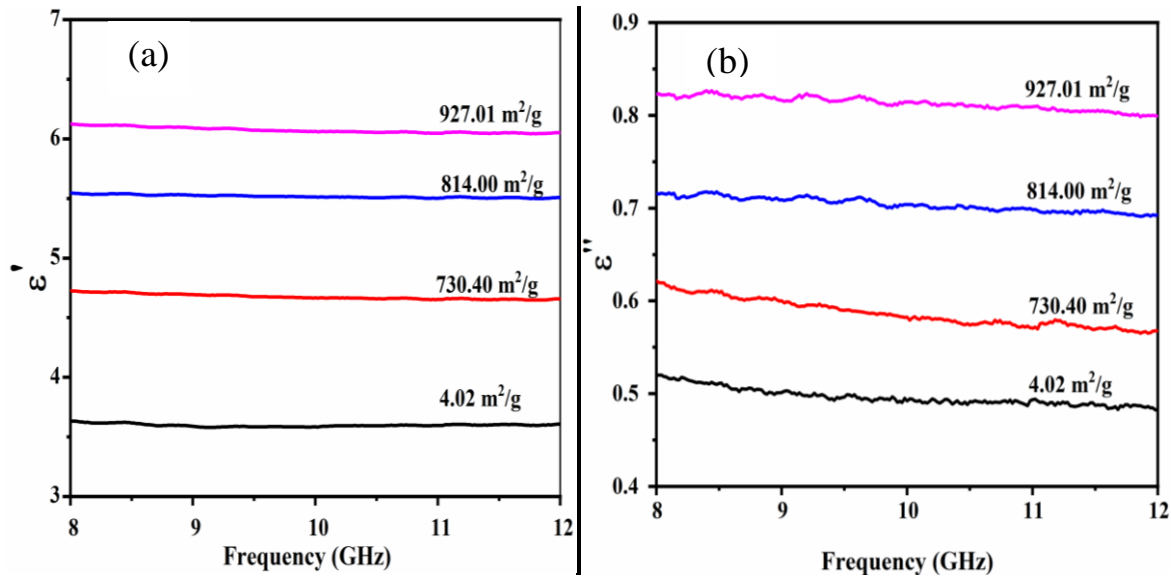


Figure 6. Variation of (a) dielectric constant and (b) loss factor with frequency for different AC surface area

Material Absorption Properties

The effect of activation treatment on the absorbing properties of AC was studied based on FEM simulations. Figure 7 shows the frequency variation of $|S_{21}|$ (dB) and demonstrates the effect of increased surface area on the attenuation properties of the activated OPEFB fiber. The graphs showed that the higher the surface area, the higher the absorption values, which indicated a greater attenuation from the absorption of the material. The $|S_{21}|$ relied on the complex permittivity values and hence the higher ϵ'' values of the AC might have resulted in higher electromagnetic energy absorption leading to lower (dB).

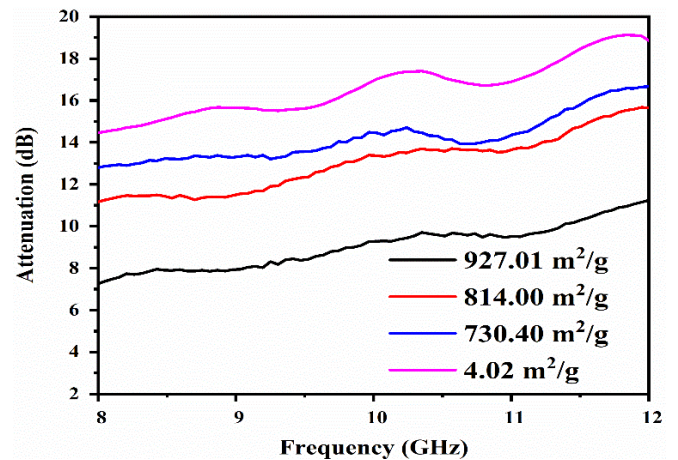


Figure 7. Variation of modified OPEFB fiber with frequency for different AC surface area

FEM simulation results of the electric field (V/m) distribution at the X-band frequency of the microstrip covered with modified OPEFB fiber is illustrated in Figure 8. The decrease in the propagating wave intensity from port 1 to port 2 (input to output) as the surface area was increased agrees with the simulated $|S_{21}|$ (dB) results. As expected, the greater loss material absorbs more light and hence transmits fewer electromagnetic waves through the sample (Mensah *et al.*, 2019).

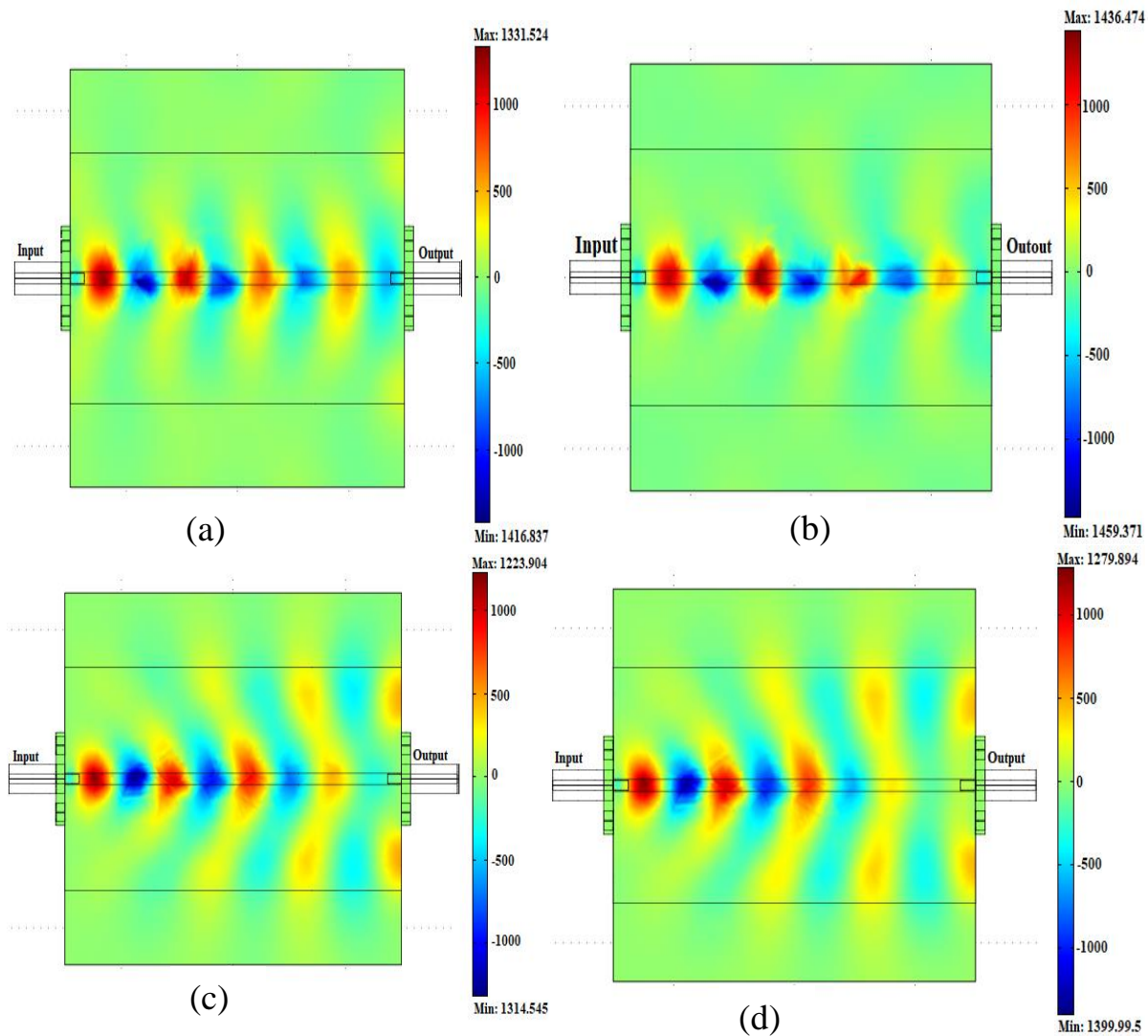


Figure 8. Electric field distribution patterns for AC of (a) 4.02 m²/g, (b) 730.40 m²/g, (c) 814.00 m²/g and (d) 927.01 m²/g

Conclusions

The complex permittivity of activated carbons synthesized from OPEFB fiber was increased significantly after increasing the surface area of the precursor through physical activation for several temperatures. Surface morphology defects and disorders, that took place in the activated samples as the surface area increased, stimulated the enhancements in the electromagnetic properties of the activated carbons. The simulated $|S_{21}|$ (dB) properties shown by the ACs have verified their tendency to attenuate microwaves at X-band frequencies. The significant dielectric properties of AC associated with particle size and surface area can be used in areas demanding adjustable attenuation of electromagnetic energy. Activated carbons with enhanced dielectric properties are cheaper to manufacture, lighter and may lessen the drawbacks related to Metallic fillers such as ferrites widely used in microwave absorption.

Acknowledgment

This work was supported by Universiti Putra Malaysia Grants (Putra initiative Grants (UPM/700-1/2/GPPI/2017/954160)), Impact Putra Grants (GP-IPS/2017/9580600) and the Ministry of Education Malaysia (Fundamental Research Grants Scheme (FRGS) (No. 5524942).

Declaration

All the data analyzed during the current study are presented in the manuscript

Conflict of interest; The authors declare no conflict of interest

REFERENCES

- Abdalahadi, D. M., Abbas, Z., Ahmad, A. F., Matori, K. A., & Esa, F. (2018). Controlling the Properties of OPEFB/PLA Polymer Composite by Using Fe₂O₃ for Microwave Applications. *Fibers and Polymers*, 19(7), 1513-1521.
- Afifah Mahmud, N., Osman, N., & Jani, A. M. M. (2018). Characterization of Acid Treated Activated Carbon From Oil Palm Empty Fruit Bunches (EFB). *JPhCS*, 1083(1), 012049.
- Ahmed, M. J. (2016). Application of agricultural based activated carbons by microwave and conventional activations for basic dye adsorption. *Journal of Environmental Chemical Engineering*, 4(1), 89-99.
- Chayid, M. A., & Ahmed, M. J. (2015). Amoxicillin adsorption on microwave prepared activated carbon from *Arundo donax* Linn: isotherms, kinetics, and thermodynamics studies. *Journal of Environmental Chemical Engineering*, 3(3), 1592-1601.
- Choh, J. L., Ching, Y. C., Gan, S. N., Rozali, S., & Julai, S. (2016). Effects of oil palm empty fruit bunch fiber on electrical and mechanical properties of conductive filler reinforced polymer composite. *BioResources*, 11(1), 913-928.
- El Khaled, D., Novas, N., Gazquez, J.A. and Manzano-Agugliaro, F., 2018. Microwave dielectric heating: Applications on metals processing. *Renewable and Sustainable Energy Reviews*, 82, pp.2880-2892.
- Ibrahim Lakin, I., Abbas, Z., Azis, R.S. and Abubakar Alhaji, I., 2020. Complex Permittivity and Electromagnetic Interference Shielding Effectiveness of OPEFB Fiber-Polylactic Acid Filled with Reduced Graphene Oxide. *Materials*, 13(20), p.4602.
- Ibrahim Lakin, I., Abbas, Z., Azis, R. S., Ibrahim, N. A., & Abd Rahman, M. A. (2020). The Effect of MWCNTs Filler on the Absorbing Properties of OPEFB/PLA Composites Using Microstrip Line at Microwave Frequency. *Materials*, 13(20), 4581.
- Lee, T., Matsumoto, A., Othman, R., & Yeoh, F. Y. (2013). Activated carbon fiber derived from pyrolysis of palm fiber. In *Advanced Materials Research* (Vol. 686, pp. 92-103). Trans Tech Publications Ltd.
- Lee, T., Zubir, Z.A., Jamil, F.M., Matsumoto, A. and Yeoh, F.Y., 2014. Combustion and pyrolysis of activated carbon fibre from oil palm empty fruit bunch fibre assisted through chemical activation with acid treatment. *Journal of Analytical and Applied Pyrolysis*, 110, pp.408-418.
- Mensah, E. E., Abbas, Z., Azis, R. A. S., Ibrahim, N. A., & Khamis, A. M. (2019). Complex Permittivity and Microwave Absorption Properties of OPEFB Fiber-Polycaprolactone Composites Filled with Recycled Hematite (α -Fe₂O₃) Nanoparticles. *Polymers*, 11(5), 918.
- Mensah, E. E., Abbas, Z., Azis, R. A. S., & Khamis, A. M. (2019). Enhancement of Complex Permittivity and Attenuation Properties of Recycled Hematite (α -Fe₂O₃) Using Nanoparticles Prepared via Ball Milling Technique. *Materials*, 12(10), 1696.
- Ooi, C. H., Ang, C. L., & Yeoh, F. Y. (2013). The properties of activated carbon fiber derived from direct activation from oil palm empty fruit bunch fiber. In *Advanced Materials Research* (Vol. 686, pp. 109-117). Trans Tech Publications Ltd.
- Ooi, C. H., Cheah, W. K., Sim, Y. L., Pung, S. Y., & Yeoh, F. Y. (2017). Conversion and characterization of activated carbon fiber derived from palm empty fruit bunch waste and its kinetic study on urea adsorption. *Journal of environmental management*, 197, 199-205.
- Osman, N. B., Shamsuddin, N., & Uemura, Y. (2016). Activated carbon of oil palm empty fruit bunch (EFB); core and shaggy. *Procedia engineering*, 148, 758-764.
- Ratan, J. K., Kaur, M., & Adiraju, B. (2018). Synthesis of activated carbon from agricultural waste using a simple method: Characterization, parametric and isotherms study. *Materials Today: Proceedings*, 5(2), 3334-3345.
- Sherif, E. S. M., Mohammed, J. A., Abdo, H. S., & Almajid, A. A. (2016). Corrosion behavior in highly concentrated sodium chloride solutions of nanocrystalline aluminum processed by high energy ball mill. *International Journal of Electrochemical Science*, 11(2), 1355-1369.
- Srivastava, S.K. and Manna, K., 2022. Recent Advancements in Electromagnetic Interference Shielding Performance of Nanostructured Materials and their Nanocomposites: A Review. *Journal of Materials Chemistry A*.
- Tsubota, T., Morita, M., Kamimura, S., & Ohno, T. (2016). New approach for synthesis of activated carbon from bamboo. *Journal of Porous Materials*, 23(2), 349-355.
- Wirasnita, R., Hadibarata, T., Yusoff, A. R. M., & Lazim, Z. M. (2015). Preparation and characterization of activated carbon from oil palm empty fruit bunch wastes using zinc chloride. *Jurnal Teknologi*, 74(11), 77-81.
- Yakubu, A., Abbas, Z., Esa, F., & Tohidi, P. (2015). The effect of ZnO nanoparticle filler on the attenuation of ZnO/PCL nanocomposites using microstrip line at microwave frequency. *International Polymer Processing*, 30(2), 227-232.
- Yang, H., Ye, T., Lin, Y., Zhu, J., & Wang, F. (2016). Microwave absorbing properties of the ferrite composites based on graphene. *Journal of Alloys and Compounds*, 683, 567-574.
- Zhong, L., Zhang, Y., Ji, Y., Norris, P., & Pan, W. P. (2016). Synthesis of activated carbon from coal pitch for mercury removal in coal-fired power plants. *Journal of Thermal Analysis and Calorimetry*, 123(1), 851-860.